Geomorphology 281 (2017) 66–77

Contents lists available at ScienceDirect

Geomorphology

journal homepage: www.elsevier.com/locate/geomorph

Modeling rockfall frequency and bounce height from three-dimensional simulation process models and growth disturbances in submontane broadleaved trees

Christophe Corona [a,*], Jérôme Lopez-Saez [b], Adrien Favillier [a], Robin Mainieri [c], Nicolas Eckert [c], Daniel Trappmann [d], Markus Stoffel [d,e,f], Franck Bourrier [b], Frédéric Berger [b]

[a] Centre National de la Recherche Scientifique (CNRS), UMR 6042, GEOLAB, 63057 Clermont-Ferrand Cedex, France
[b] Université Grenoble Alpes, Irstea, UR EMGR, 2 rue de la Papeterie, BP76, F-38402 St-Martin-d'Hères, France
[c] Université Grenoble Alpes, Irstea, UR ETNA, 2 rue de la Papeterie, BP76, F-38402 St-Martin-d'Hères, France
[d] University of Bern, Institute of Geological Sciences, CH-3012 Berne, Switzerland
[e] University of Geneva, Institute for Environmental Sciences, Climatic Change and Climate Impacts, 66 Boulevard Carl-Vogt, CH-1205 Geneva, Switzerland
[f] University of Geneva, Department of Earth Sciences, 13 rue des Maraîchers, CH-1205 Geneva, Switzerland

ARTICLE INFO

Article history:
Received 10 June 2016
Received in revised form 20 December 2016
Accepted 20 December 2016
Available online 24 December 2016

Keywords:
Forest-rockfall interactions
Scar-counting approach
3D process based simulation model
Rockfall simulation
French Alps

ABSTRACT

The use of dynamic computational methods has become indispensable for the assessment of rockfall hazards and the quantification of uncertainties. Although a substantial number of models with various degrees of complexity has become available over the past few years, models have only rarely been parameterized against observations, especially because long-term records of rockfalls have proven to be scarce and typically incomplete. On forested slopes, tree-ring analyses may help to fill this gap, as they have been shown to provide annually resolved data on past rockfall activity over long periods. In this paper, a total of 1495 rockfall scars recorded on the stem surface of 1004 trees have been studied at a site in the Vercors massif (French Alps) to calibrate the 3D process based simulation model RockyFor3D. Uncertainties related to the choice of parameters accounting for energy dissipation and surface roughness have been investigated in detail. Because of the lack of reliable data, these parameters typically are estimated based on expert judgments, despite the fact that they have significant impacts on runout distances and bounce height. We demonstrate that slight variations in roughness can indeed strongly affect the performance of runout modeling and that the decreasing downward gradient, observed in field data, is properly reproduced only if reduced roughness (<10 cm) enables blocks to reach the distal parts of the study plot. With respect to the height of impacts, our results also reveal that differences between simulations and observations can indeed be minimized if softer soil types are preferred during simulation, as they typically limit bouncing. We conclude that field-based dendrogeomorphic approaches represent an objective tool to improve rockfall simulations and to enhance our understanding of parameterization, which is of key importance for process dynamics and thus hazard zoning.

1. Introduction

Rockfall is a widespread phenomenon in mountain environments where it threatens human beings and poses significant challenges to infrastructure, industry and housing (Volkwein et al., 2011). Despite the fact that the process itself usually involves rather limited volumes, rockfall phenomena can nevertheless result in economic losses due to service interruptions and equipment damage, as well as to injury or death of users and operators of these facilities. As a consequence, rockfall protection via both structural and land use planning actions is an important issue for administrators and stakeholders in areas affected by rockfall (Agliardi et al., 2009). Basically, the design of protection measures and rockfall hazard zoning require data on three basic characteristics of rockfalls, namely the number of passing rocks per time unit, impact energy, and impact height. That is, information is required on the mass and velocity of the fall to determine the energy capacity and on the location of impact points, trajectory paths, and runout distances so as to determine danger zonation or the optimum location and dimensioning of defense structures (e.g., barriers or fences; Jaboyedoff et al., 2005). However, predicting the rockfall runout distance and propagation areas, i.e., the areas potentially threatened by rockfall, is still a challenge (Jaboyedoff and Labiouse, 2011). Over the last decades, many kinematic computer modeling programs have been made available to

* Corresponding author.
E-mail address: christophe.corona@univ-bpclermont.fr (C. Corona).

http://dx.doi.org/10.1016/j.geomorph.2016.12.019
0169-555X/

simulate rockfall behavior (Crosta and Agliardi, 2004), but their reliability has been shown to depend chiefly on a thorough understanding of impact mechanics and trajectory analysis and on the availability of precise data on past rockfalls to calibrate the models (Volkwein et al., 2011; Bourrier and Hungr, 2013).

At larger scales, model outputs can be evaluated statistically by using documentation of past rockfalls (e.g., Dussauge, 2003). For more detailed studies and at the slope scale, however, inventory data will remain unavailable, scarce, or unreliable in most cases and will thus prevent the application of statistical approaches. This is even more so the case in remote areas and for low-magnitude events that have not caused damage in the past (Corominas and Moya, 2010; Trappmann et al., 2014). Another possibility to evaluate model reliability is the long-term, real-time observation of cliffs, but such data do not normally exist either as they are very time consuming and only available (if at all) for small sites and for a short period of time (Matsuoka and Sakai, 1999).

Over the last decades, the inclusion of rockfall trajectory frequencies as obtained from tree-ring records (Stoffel et al., 2010; Stoffel and Corona, 2014) have been used to close this data gap and to assist the validation of trajectory frequency maps derived from simulations (Stoffel et al., 2006). More recently, Corona et al. (2013) demonstrated that impact data on trees can facilitate the characterization of input parameters of rockfall models, such as the delineation of active source areas of rockfalls. The inclusion of dendrogeomorphic rockfall records was also used in the past to transform modeled trajectory frequencies into real rockfall frequencies at any point on a slope under investigation (Trappmann et al., 2013, 2014).

With the aim of improving rockfall hazard studies for environmental management purposes and to further optimize analyses, this paper proposes a methodology for the assessment of rockfall model input parameters by coupling field-based impact data (i.e., scar count and impact height determination) from broadleaved trees with three-dimensional (3D), process-based rockfall modeling approaches. Field data were gathered through an exhaustive and systematic mapping of 1004 submontane broadleaved trees from a 0.6-ha plot containing 1495 scars visible on the tree stem surface. This data set was then compared to the results of 16 sets of simulation runs performed with the probabilistic, process-based rockfall trajectory model RockyFor3D. We demonstrate that the rockfall model is highly sensitive to parameters associated with soil properties and slope surface and any changes thereof. We also illustrate how differences between modeling and dendrogeomorphic reconstructions can be minimized through a careful calibration of soil mechanical properties and slope surface roughness.

2. Study site - geologic setting and rockfall triggering mechanisms

The study site, a locality known as «Croupe du Plantin» (45°05′02″N, 5°39′16″E, 470–630 m asl) is situated on the eastern slopes of the Vercors massif (French Alps, Fig. 1A), on the territory of the village of Saint-Paul-de-Varces (2500 inhabitants). Rockfall originates from a ~30-m-high, south east-facing cliff consisting of Valanginian limestones and marls, where narrow jointing, roughly characterized by subhorizontal bedding and subvertical orthogonal joints, favors considerable fragmentation and the release of small rock fragments with volumes ranging from a few dm^3 to 1 m^3 (Fig. 1B).

According to a high-resolution DEM derived from airborne LiDAR data, Quaternary rockfalls have formed an ~240-m-long talus slope with a downslope gradient ranging from 39° to 25° bordered by two interfluves (Favillier et al., 2015). At the apex of the talus, slope morphology is characterized by a slight depression (depth ~2 m) separating the study plot into two ~30-m-wide couloirs that tend to channelize falling rock fragments in their downslope movement (Fig. 1C, D). The tree plot analyzed here has an area of 0.6 ha (120 × 50 m) and is covered by a dense (~2000 trees·ha^{-1}) forest stand predominantly composed of *Acer opalus* subsp. *opalus* (Italian maple) and *Quercus pubescens* subsp. *pubescens* (pubescent oak) mixed with *Sorbus aria* (L.) Crantz (common whitebeam), *Acer campestre* subsp. *Leiocarpum* (field maple), and *Fraxinus excelsior L.* subsp *excelsior* (common ash) (Fig. 2). Frequent scars on the stem surface are clear evidence of the presence of regular rockfall activity (Fig. 1E, F).

Whereas the cause of a rockfall is ultimately related to weathering, fracturing, and erosion of rocks, the actual trigger that causes a rock to become unstable and fall is often difficult to ascertain. Mean annual precipitation (1961–2013) at the nearest meteorological station, Grenoble (45°09′58″N, 5°45′58″E, 220 m asl), located 10 km northeast of the study site, is 934 mm. Mean annual temperature is 12.5 °C with 64 days experiencing freezing. Rock fragments are dislodged from the cliff along preexisting or new discontinuities, and the triggering mechanisms of rockfalls include freeze–thaw cycles of interstitial water

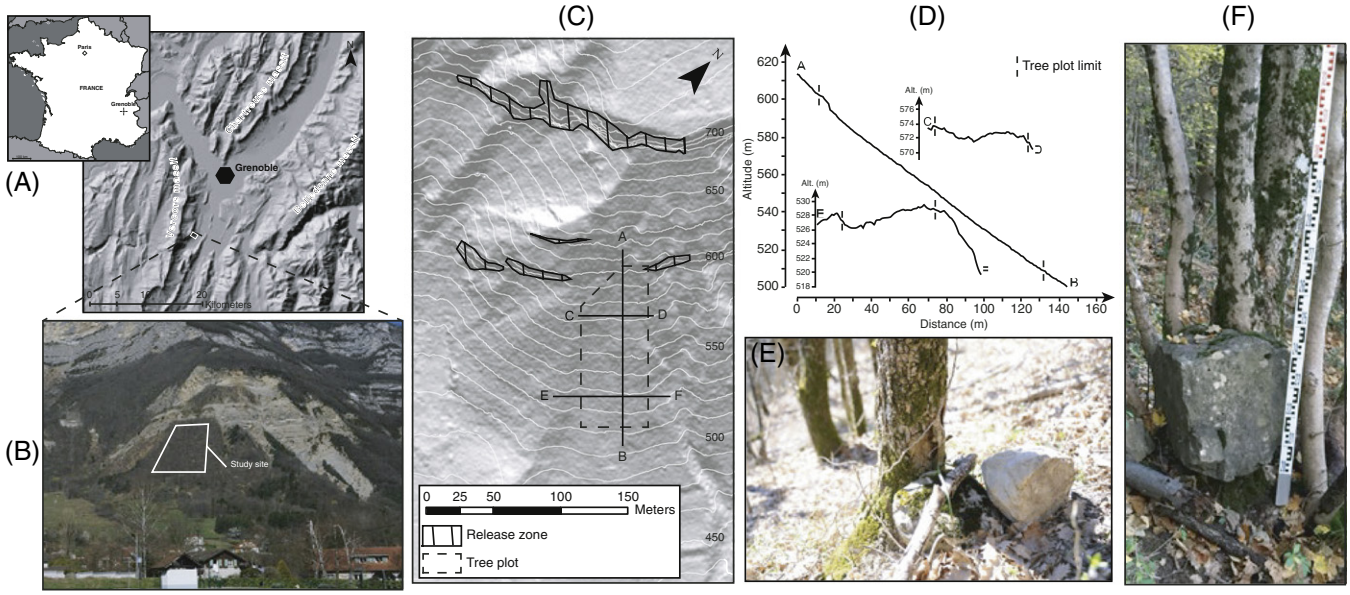

Fig. 1. Overview of the study site. The study site is located in the French Alps (A), on the eastern slopes of the Vercors massif, 20 km southwest of Grenoble. (B) The study plot (delimited by a white polygon) is dominated by a ~30-m-high, south east-facing cliff built of Valanginian limestones. (C) Hillshade map built from a DEM derived from airborne LiDAR data. (D) Longitudinal and lateral profiles of the slope under investigation. (E, F) Illustration of injured *Acer opalus* in the forest stand.

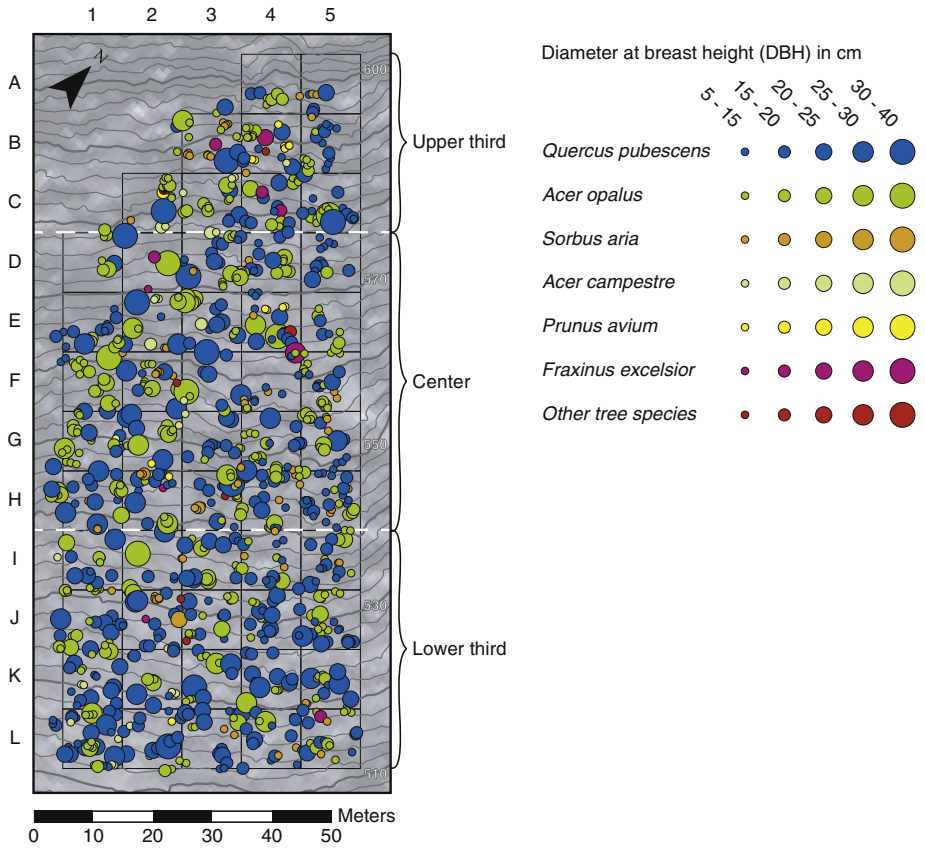

Fig. 2. Spatial distribution and diameters at breast height (DBH; in cm) of trees in the study plot.

(Matsuoka and Sakai, 1999), snowmelts as well as intense rainfall (Cardinali et al., 2006). Historical and instrumental seismicity rates are low, and the possible role of earthquakes triggering rockfalls (Dussauge, 2003) is not indicated.

The municipality of Saint-Paul-de-Varces is severely exposed to rockfall hazards. Two major collapses have been reported in historical archives, one at the beginning of the seventeenth century and another one in December 2008, the latter having a volume estimated to 1625 m^3 (Hantz et al., 2014). Vulnerability of the settlement to rockfall has increased rapidly since the 1950s, owing to the rapid periurban expansion of settlements in the wider Grenoble region (Astrade et al., 2007). As a consequence, rockfall hazard assessments have become a key concern for local stakeholders and policy makers.

3. Material and methods

The 'Croupe du Plantin' tree plot was selected as (i) past rockfalls have left numerous visible impacts on tree stems, (ii) no other geomorphic processes caused injuries to trees, and (iii) the forest was not exploited over the last century. On this slope, the recorded rockfall frequency was evaluated with a three-step procedure including the (i) scar-counting approach on a tree sample plot as described by Trappmann and Stoffel, (2013) or Favillier et al. (2015); (ii) modeling rockfall trajectories using RockyFor3D (v5.0; Dorren, 2012), a probabilistic process-based rockfall trajectory model; and (iii) the comparison of the observed and modeled distributions of rockfall passages in terms of frequency and height.

3.1. Tree plot and scar-counting approach

At the study site, virtually all trees show visible growth anomalies on the stem surface resulting from past rockfalls, predominantly in the form of injuries. As scars represent the most accurate and reliable growth disturbance (GD) to date past rockfalls in tree-ring records (e.g., Schneuwly et al., 2009a,b; Stoffel et al., 2013), we actively searched for visible stem wounds at the study site. To precisely assess the spatial and temporal patterns of past rockfall activity, trees with a diameter at breast height (DBH) >5 cm were systematically mapped in a 50 × 120 m tree plot orientated perpendicular to the line of maximum slope gradient (Fig. 2). The position of each tree was determined (±100 cm) using a sonic rangefinder, compass, and inclinometer. All trees were positioned in a geographical information system (GIS) as geo-objects.

Trappmann and Stoffel (2013, 2015) previously demonstrated the reliability of the scar-counting approach to reconstruct spatial patterns of rockfall activity. We therefore employed this method as well, as it requires much less time and effort to estimate the rockfall frequency at the level of individual trees from the plot than would conventional dendrogeomorphic approaches. The latter is often time-consuming as it requires an exhaustive sampling (with cross sections and cores) and identification and cross-dating of GD forming after mechanical disturbance by rock impacts (see Trappmann and Stoffel, 2013, for more details). Recent scars were identified according to their fresh appearance, chipped bark, or injured wood (see Trappmann and Stoffel, 2015, for details). Wounds that are actively overgrowing at the time of sampling were identified based on the callus pad that is sealing the injuries from the border toward the centre (Stoffel and Perret, 2006). Older, completely healed injuries are more difficult to be detected visually; they were inferred via the occurrence of swelling and blisters on the stem surface. Extremely long, vertical scars or scars with vertical extensions <3 cm were excluded from analysis so as to avoid misclassification and/or the inclusion of injuries caused by branch breakage or falling neighbouring trees (Perret et al., 2006). The DBH distribution of trees is even over the slope (Fig. 2), such that one may also

expect a comparable distribution of tree ages across the slope and an absence of age-related biases at the slope scale. In addition to scar counting, we also measured the height of each wound (±5 cm) using a laser rangefinder.

3.2. Modelling with RockyFor3D

In a subsequent step, and on the basis of a digital elevation model (DEM; 2.5 × 2.5 m) derived from airborne LiDAR data, rockfalls at 'Croupe du Plantin' were simulated using the probabilistic, process-based rockfall trajectory model RockyFor3D (v5.0). This model combines physically based, deterministic algorithms with stochastic approaches to simulate rockfall in three dimensions and consists of three main modules. The first module calculates uniformly accelerated parabolic free fall through the air and the impacts of rocks on the slope surface against a tree (for details see Dorren et al., 2006). During each rebound, the model allows the block to deviate from its original direction before rebound so as to take account of the aspect of the terrain in which the block rebounds. The second module calculates energy loss due to impacts against trees; if an impact against a tree takes place, part of the rock's energy is dissipated as a function of the tree's diameter and of the relative position between the impacting rock and the tree's center. After a tree impact, the trajectory of a rock can be deviated laterally by up to 76° from its fall direction before the tree impact. The third module calculates the velocity of the falling rock after a rebound on the slope surface (for details see Dorren, 2012).

3.3. Delineation of release area

Input data required by RockyFor3D include, in addition to the DEM, a set of raster maps describing the (i) rockfall source cells including rock density, rock dimensions, and rock shape; (ii) mechanical properties of the surface material in each cell; and (iii) roughness of the slope surface in each cell. In addition, a tree file that contains the (iv) *x*- and *y*-coordinates of each and every single tree, as well as their stem DBH; and (v) wood type (i.e., broadleaved or conifer trees) was used to characterize the forest stand.

The morphology of a terrain displays characteristic slope angles that can be directly related to the geomorphic processes involved in slope stability; rockfall source areas are commonly found in the steepest morphological units (Michoud et al., 2012). Based on these statements, Loye et al. (2009) established a DEM-based geomorphometric approach to detect these morphological units and thereby identified rockfall source areas, approach that is also known as the Slope Angle Frequency Distribution (SAFD) procedure. In the SAFD procedure, slope angle distribution is decomposed in several Gaussian distributions that can be considered characteristic of morphological units (such as rock cliffs, steep slopes, footslopes, and plains). A terrain unit is considered a potential rockfall source if its slope angle exceeds a certain threshold, which in turn is defined where the Gaussian distribution of the morphological unit «rock cliff» becomes dominant over the «steep slope» unit. According to this analysis, and based on the Histofit routine (Loye et al., 2009), we have defined the threshold slope angle for source areas to 49° in the present case. Thereafter, potential rockfall source areas were mapped, integrated into a geographical information system (GIS), and converted to raster. The total surface of the potential release areas was evaluated to 0.41 hm^2. The rock density in each source start cell was set at 2700 $kg \cdot m^{-3}$. For all 16 sets of simulations performed in this study, the initial fall height of rocks in the rockfall start cells was set to 2 m. To obtain sufficiently stable outputs, each set of simulation was performed with 10,000 simulated blocks from each of the 664 source cells, resulting in a total number of 6,640,000 simulated trajectories.

3.4. Simulations setup

In the transit area of rockfall (i.e., the zone located between the source and depositional area), the systematic tree inventory was used as a tree file to characterize the forest stand. In this area, Rockyfor3D uses a normal and a tangential coefficient of restitution to calculate rock rebound on the slope surface (Volkwein et al., 2011). The normal coefficient of restitution (*rn*) defines the change in normal velocity during impact. In Rockyfor3D, *rn* values are associated with slope materials and consequently depend on their mechanical properties, i.e., the capacity of slope materials to dissipate energy in particular. The tangential coefficient of restitution (*rt*) defines the reduction in tangential velocity during impact. Both coefficients depend on (i) the rock shape and radius, (ii) the depth of the impact crater during a rebound (i.e., the soil strain conditioned by the soil type in other words), and (iii) the roughness of the slope surface (Dorren et al., 2005). Based on field observations and fresh rockfall measurements, square blocks of 0.064 m^3 (0.4 × 0.4 × 0.4 m) were used for simulations. According to Bourrier and Hungr (2013) and Gischig et al. (2015), surface roughness and soil mechanical energy dissipation capacity are crucial and explain much of the differences between the various models available on the market as they influence the periodic contacts (impacts) between the particle and the slope substrate. Usually, however, both quantities are difficult to measure with precision. As a result, they are estimated based on field observations and expert. In this study, 16 sets of simulations were computed to account for four different soil structures (i.e., from fine soil material with a depth >~100 cm to talus slope with rock fragments Ø >~10 cm, which corresponds to *Rn* values in the range of 0.21–0.42) and four roughness values defined in three raster maps (rg70, rg20, and rg10) corresponding to the height of a representative obstacle that a falling block encounters in respectively 70%, 20%, and 10% of the cases during a rebound. The characteristics of each set of simulations are summarized in Table 1.

3.5. Comparison between observations and simulations

Results from the 16 simulation sets and the dendrogeomorphic analysis were compared on the basis of the spatial distribution of rockfall impacts on trees, as the latter has been demonstrated to be a good indicator for the spatial distribution of rockfall trajectories (Trappmann et al., 2014). However, and as a result of the large number of simulations, the sum of simulated impacts on trees greatly exceeds the number of scars observed in nature (scar-counting approach). A normalized

Table 1
Overview on the soil type and roughness parameters used for the simulations.

Simulation parameters Simulation	Soiltype	Roughness 70%/20%/10%
S1	1	0.00/0.00/0.00
S2	2	0.00/0.00/0.00
S3	3	0.00/0.00/0.00
S4	4	0.00/0.00/0.00
S5	1	0.00/0.05/0.10
S6	2	0.00/0.05/0.10
S7	3	0.00/0.05/0.10
S8	4	0.00/0.05/0.10
S9	1	0.05/0.10/0.20
S10	2	0.05/0.10/0.20
S11	3	0.05/0.10/0.20
S12	4	0.05/0.10/0.20
S13	1	0.10/0.20/0.40
S14	2	0.10/0.20/0.40
S15	3	0.10/0.20/0.40
S16	4	0.10/0.20/0.40
DEM resolution = 2.5 m Rockfall volume = 0.064 m^3 (0.4 m/0.4 m/0.4 m)		

number of simulated impacts *Nnorm* was therefore calculated for each tree (i) to render both approaches comparable:

$$Nnorm_i = \frac{(Nsimul_i * N_{scars})}{Ntotsimul} \quad (1)$$

where $Nsimul_i$ represents the number of impacts simulated at tree *i*, N_{scars} is the total number of scars obtained with field observation techniques (N_{scars} 1495) and where *Ntotsimul* gives the total number of simulated impacts.

In a subsequent step, and to visualize spatial patterns of rockfall frequency and height of impacts as well as to remove potential outliers, the number and height of impacts were clustered into 10 × 10 m cells (*n* 54). The mean number of scars and the mean height of impacts were computed at each cluster and discretized into 5 (number) and 7 (height) classes.

Comparisons between simulated and observed rockfall impact maps have been completed at the plot and cell scales. At the plot scale, distributions were produced from each map and tested for normality with the Shapiro-Wilk test. Due to their non normal distributions, the non parametric Wilcoxon-Mann-Whitney was used to compare (i) observed and simulated numbers of impacts on trees as well as (ii) mean impact heights observed in the field and modeled by RockyFor3D for the 16 sets of simulations.

At the cell scale, Cohen's kappa coefficient (Smeeton, 1985) was computed to compare the similarity of maps derived from observations and simulations. Cohen's kappa ($\varkappa$) measures the agreement between two raters (i.e., observations and models in our case) that each classify *N* items (cells) into *C* mutually exclusive classes defined according to the distribution of recurrence intervals and height of impacts as:

$$\varkappa = \frac{\Pr(a) - \Pr(e)}{1 - \Pr(e)} \quad (2)$$

where $Pr(a)$ is the relative observed agreement among observations and simulations, and $Pr(e)$ is the hypothetical probability of chance

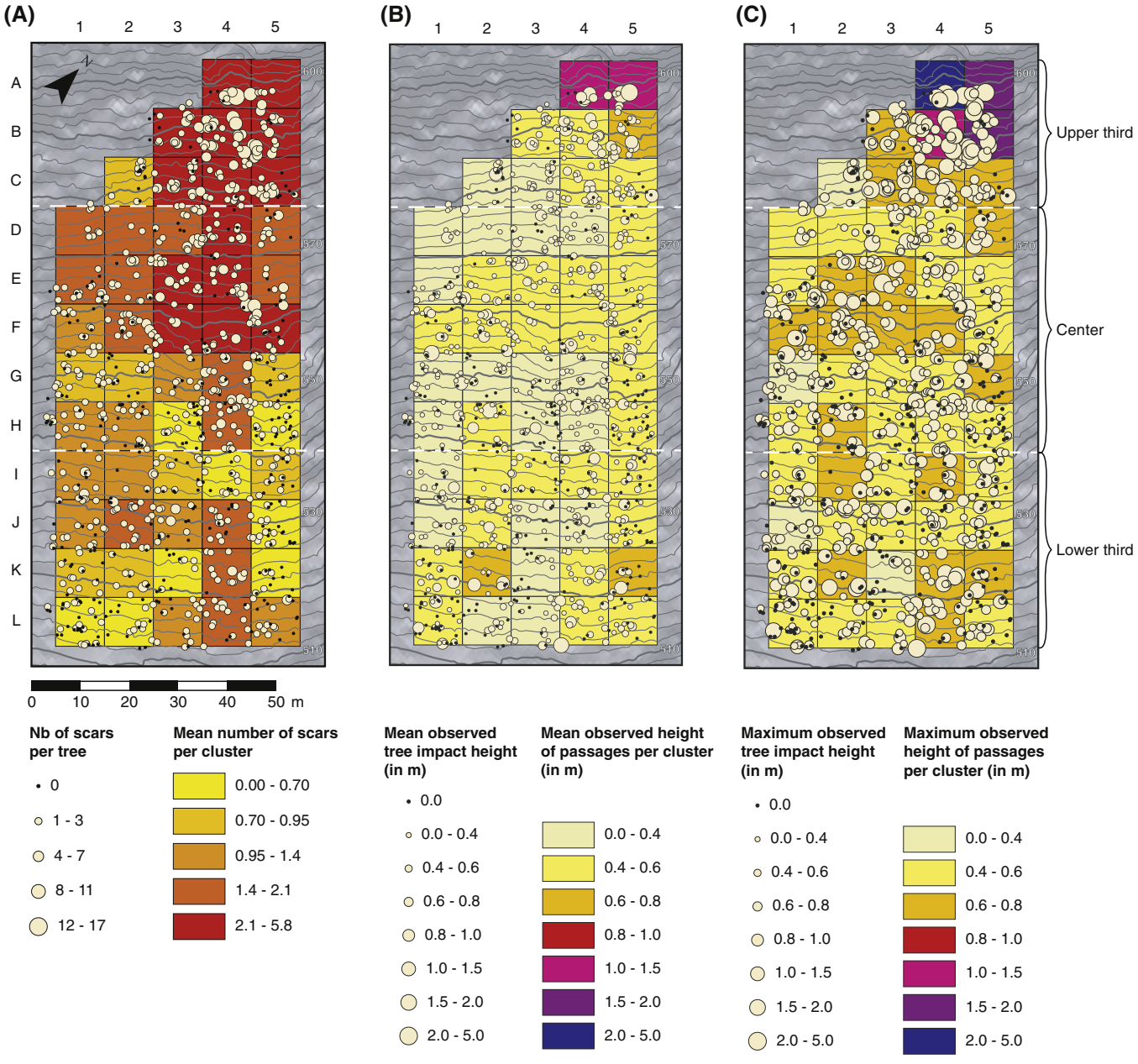

Fig. 3. Spatial distribution of the (A) 1495 observed scars (1004 trees) as well as (B) mean and (C) maximum impact heights per tree.

agreement, using the observed data to calculate probabilities of each species distributed randomly in each class of recurrence interval. According to Landis and Koch (1977), $\varkappa$ values <0 indicate no agreement, 0–0.20 slight, 0.21–0.40 fair, 0.41–0.60 moderate, 0.61–0.80 substantial, and 0.81–1 almost perfect agreement.

4. Results

4.1. Spatio temporal patterns of rockfall activity revealed by the scar-counting approach

At the plot scale, a total of 1004 trees was mapped (mean DBH: 14.6 ± 6.2 cm) amongst which a majority of *Quercus pubescens* Willd. (*Qp*, *n* 441, 52.1%, mean DBH: 17.6 ± 5.9 cm) and *Acer opalus Mill.* (*AO*, *n* 406, 47.9%, mean DBH: 13.2 ± 6.1 cm) trees; trees of these species were heterogeneously distributed in the cells (Fig. 3). Based on the scar-counting approach, 1495 scars were recorded on the stem surfaces. The mean number of scars per tree is 1.5 ± 1.8. A total of 331 trees (33%) did not present any visual evidence of past rockfall impacts. From a spatial perspective, the distribution of impacted trees exhibits a strong, decreasing trend as one moves down the slope (Fig. 3): the mean number of scars revealed by the scar-counting approach gradually decreases from an average of 2.9 ± 2.8 scars·tree^{-1} in the top third of the slope (cells A–C) to 1.5 ± 1.5 scars·tree^{-1} in the central segments of the plot (cells D–H) to reach values of 0.9 ± 1.1 in the lowest third of the plot (cells I–L). Similarly, the largest absolute number of impacts (>10 scars) was recorded in the upper half of the plot (A–F, Fig. 3A); whereas the number of stems without impacts steadily increases from 17% in the top third of the plot to 40% in its lowest third. With respect to lateral spread, the map derived from observations on 1004 trees (*Obsmap*) shows a preferential rockfall path from D1 to K1 and from A4 to L4, which is in good agreement with the topographic depressions existing in the field. Several non wounded trees in cells H3–L3 and G5–L5 are located on the interfluves, which are separating these rockfall couloirs.

The mean impact height at the slope scale is 0.6 ± 0.43 m with a maximum impact height on trees at 3.9 m. Fig. 3B and C present maps with mean and maximum impact heights, respectively. At the cluster scale, the mean height of impacts decreases from 0.63 ± 0.53 m in the top third of the slope to 0.49 ± 0.53 m in the lower one-third of the plot (Fig. 3B). When considering only the maximum impact height per tree (Fig. 3C), this decrease is even more marked as impact heights decrease from 0.86 ± 0.61 m in cells A–C to 0.54 ± 0.32 m. Fig. 4 shows the distribution of impact heights at the plot scale, in the upper (cells A–C), central (cells D–H), and lower (cells I–L) compartments of the plot. For the number of impacts and bounce height distributions, the Wilcoxon-Mann-Whitney test reveals that mean values observed in the top third compartment of the plots are statistically different from those in the bottom two-thirds ($p < 0.001$). Conversely, the distributions in the central and lowest third are comparable and the null hypothesis therefore cannot be rejected.

4.2. Spatio temporal patterns of rockfall activity revealed by the modelling approach

Accounting for uncertainties related to soil type and roughness, 16 sets of simulations (S1–S16) were successively tested in Rockyfor3D. A total of 6,640,000 rockfalls were simulated from a 0.41 hm^2 large release area with a slope angle >49°. These rockfalls caused between 28 (S13) and 567,523 (S2) impacts to the 1004 trees in the forest plot. After normalization, and irrespective of the soil parameters being used, the number of rock impacts per tree remains larger in the uppermost 40 m of the plot close to the slope apex (>2 scars per tree on average), i.e., in the vicinity of the rockfall source areas (Fig. 5). This number decreases as one moves downslope and gets closer to the bottom of the plot. Interestingly, this decreasing downward gradient is very sharp in simulations S9–S16 for which higher soil roughness (with rg10 > 5 cm, rg20 > 10 cm, and rg70 = 20 cm) was assumed. As a consequence, and using these scenarios, almost no impacts are recorded in the bottom half of the plot (cells F to L). Conversely, for S1–S8, characterized by smoother soil micro topography (rg10 = 0, rg20 < 5 cm, and rg70 < 0.1), the mean number of virtual scars ranges between ~1 and >2 impacts per tree at the outlet of both couloirs (L2–L4).

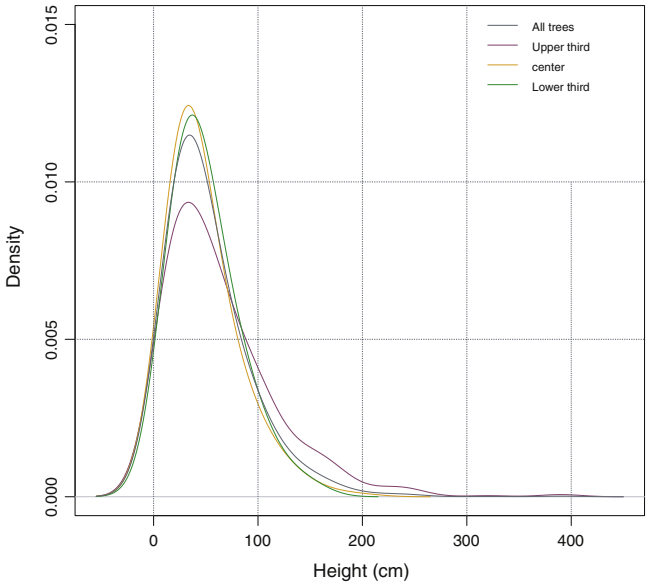

Fig. 4. Probability density functions of mean impact heights for the three compartments of the study plot as derived with the scar-counting approach.

The maps illustrating mean impact heights (Fig. 6) shows a clear decreasing downslope gradient with a mean height of passages that exceed 0.8 m only in cells A–C. By contrast, bounce heights only rarely reach 0.8 m in the lowermost part of the plot (K–L). In more detail, the gradient is sharper for S1, S5, S9, and S13-S16, corresponding either to higher roughness parameters (0.1, 0.2, 0.4 m for rg70, rg20, and rg10, respectively) or to soil type '1' (i.e., soil constituted of fine material with depth >100 cm) in which rockfall passages never exceed 0.4 m in the lowest third of the plot.

4.3. Comparison of observed and modeled rockfall impacts

In a first step, agreement between observed and modeled numbers of rockfall impacts has been investigated using distributions at the plot scale for the 16 sets of simulations (Fig. 7). According to the Wilcoxon-Mann-Whitney test, simulated distributions of rockfall impacts on trees are similar to observations for S1–S4 and S6–S8 (Table 2). On the other hand, for simulations S5 and S9–S16, the null hypothesis has to be rejected ($p < 0.05$), meaning that the distributions of the number of impacts in these latter runs differ statistically from our field observations. Comparing the agreement of observed and modeled maps at the scale of raster cells, the K-Cohen coefficients reveal that maps obtained from simulations S1–S8, S11–S12, and S16 are in fair agreement (K > 0.1) with the scar-counting approach and should be preferred over other simulations for which a complete absence of agreement was obtained (Table 2).

In a second step, the distributions of mean modeled impact heights on trees have been compared to field observations for the 16 sets of simulations (Fig. 8). At the plot scale, the Wilcoxon-Mann-Whitney tests point to a convergence ($p < 0.05$) between observed and simulated distributions of mean impact heights for simulations S2 and S7–S8. No convergence is observed between observations and simulations for the other sets of simulations (Table 2). With regard to the spatial

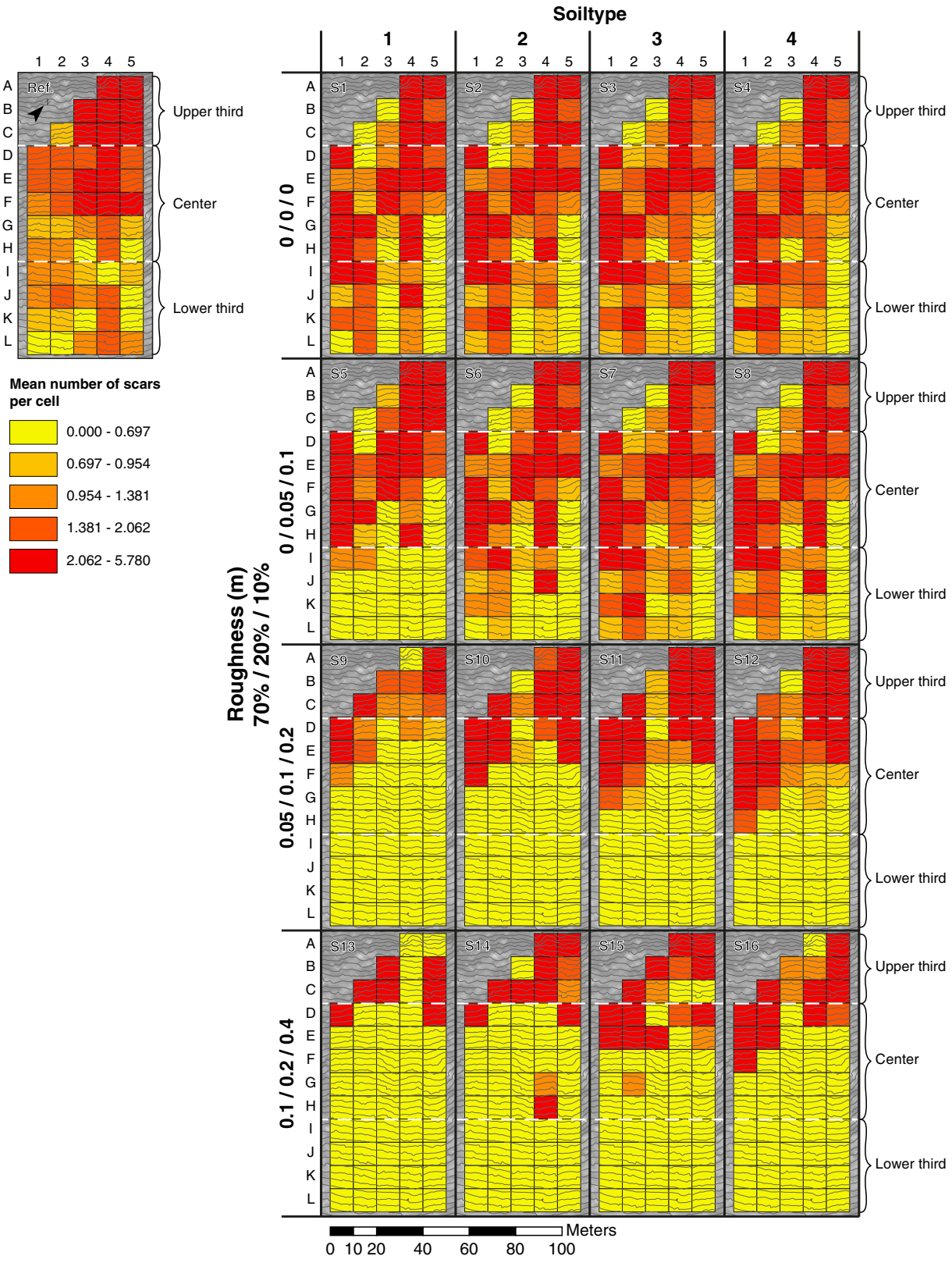

Fig. 5. Comparison between the spatial distribution (upper left map) of observed scars and simulated impacts for the 16 sets of simulations named S1–S16.

distribution of impact heights, Cohen's K coefficients remain lower than in the rockfall frequency assessment, yet slight agreement ($0.1 < k < 0.2$) is observed between mean observed and simulated impact heights for S1, S6–S7, S10, and S12.

Finally, taking into account the number and height of impact distributions, the sets of simulations S5 and S9–S16 appear fairly unrealistic due to the absence of convergence between observations and simulations for both variables (Table 2). By contrast, S1, S3–S4, and S6 appear

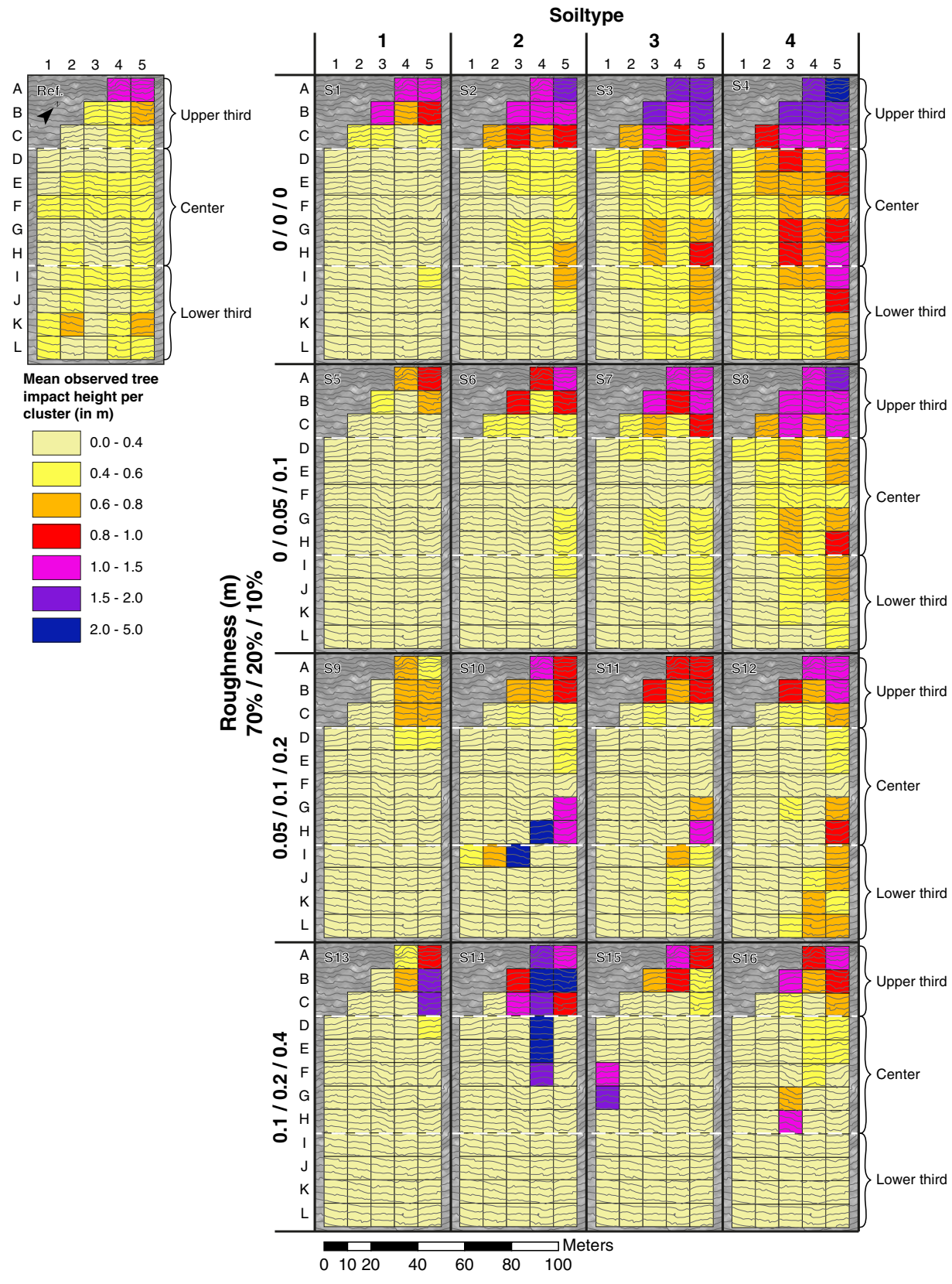

Fig. 6. Comparison between the spatial distribution (upper left map) of mean observed and simulated impact heights for the 16 sets of simulations (S1–S16).

more reliable as significant similarities were found for the observed and simulated rockfall frequencies. Finally, S7 and S8 can be considered as the most reliable simulations as convergences were computed for the number and for the height of rockfall impacts.

5. Discussion

The use of dynamic computational methods has become indispensable when it comes to the assessment of rockfall hazards and risks.

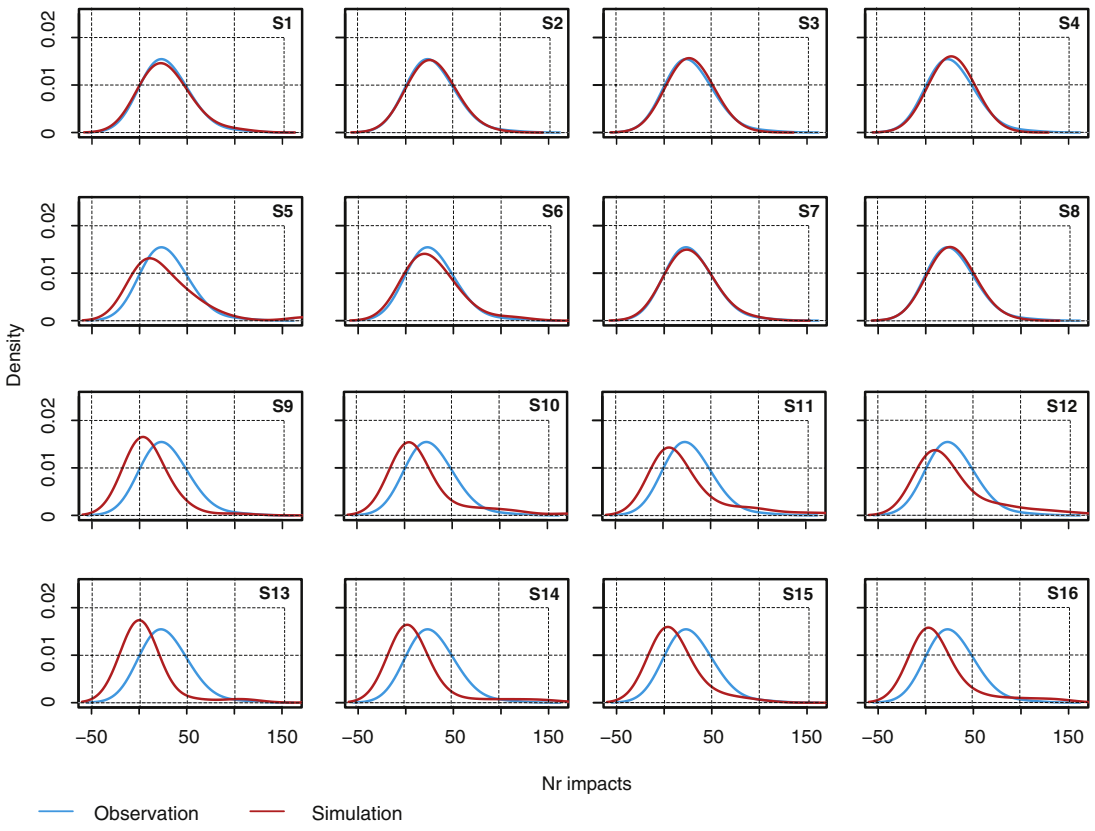

Fig. 7. Probability density functions of the number of impacts per tree in the observational data set (blue curve) and for simulations S1–S16 (red curves).

Although a number of models with various degrees of complexity are currently available, we realize that model parameters have only rarely been calibrated against historical series. This is mainly because long-term records of rapid mass movements, such as rockfalls, have proven to be quite limited if not available at all (Gischig et al., 2015). This absence of calibration is very problematic in urbanized areas where the number of events increases in proportion to urbanization (Volkwein et al., 2011; Michoud et al., 2012), with direct implications on rockfall risk and related loss potential. In these areas, a search for methods that allows precise and reliable reconstruction of past rockfall activity - and subsequent calibration of models - is urgently needed. In the case that such critical slopes are forested, dendrogeomorphology has proven to be a reliable approach as it allows reconstruction of past rockfall activity in the absence of inventory data or clear morphological evidence, as is often the case on scree slopes or in the case of isolated, yet undated blocks (Favillier et al., 2015). Despite this potential, information derived from tree-ring techniques has rarely been used for the calibration of dynamic models, with the exception of a few studies dedicated to the detection of potential release areas (Corona et al., 2013) or the association of real frequencies in modeled trajectories (Trappmann et al., 2014). In this study, we combined the dendrogeomorphic and the modeling approaches. Here, we used scar counts derived from dendrogeomorphic analysis to (i) assess model parameters of RockyFor3D as well as to (ii) test its capability to accurately predict rockfall patterns on a forested slope.

Table 2
Wilcoxon-Mann-Whitney p-values and Kappa Cohen indices. Wilcoxon-Mann-Whitney p-values and Cohen's kappa coefficient have been computed between rockfall distributions and maps derived from field inventory and sets of simulations (S1–16) with regard to the number of impacts and mean height of impacts.

	p-Value (Wilcoxon-Mann-Whitney test)		Cohen's kappa coefficient	
Simulations	Obs. Nr passages vs sim. Nr passages	Obs. mean height vs sim. mean height	Obs. Nr passages vs sim. Nr passages	Obs. mean height vs sim. mean height
S1	0.837	0.000	0.15	0.10
S2	0.832	0.060	0.20	0.06
S3	0.701	0.000	0.22	0.04
S4	0.625	0.000	0.17	−0.05
S5	0.040	0.000	0.28	0.09
S6	0.493	0.000	0.19	0.14
S7	1.000	0.102	0.18	0.12
S8	0.766	0.101	0.22	0.04
S9	0.000	0.000	0.06	0.07
S10	0.000	0.000	0.07	0.11
S11	0.000	0.000	0.16	0.09
S12	0.011	0.005	0.13	0.12
S13	0.000	0.000	0.07	0.07
S14	0.000	0.000	0.09	0.09
S15	0.000	0.000	0.08	0.08
S16	0.000	0.000	0.09	0.09

Uncertainties related to energy dissipation (i.e., soil type) and surface roughness have been calibrated in detail in this study as they affect (i) the energy loss of the falling block due to the penetration depth into slope material and (ii) the runout distance of blocks. For this purpose, 16 different sets of scenarios have been successively compared to rockfall patterns derived from an exhaustive mapping and the systematic counting (Trappmann and Stoffel, 2013) of visible scars on tree stems in a 0.6-ha plot. The distributions extracted from simulations S1–S4 and S6–S8 compare nicely with observations, insofar the number of impacts per stem at the plot scale is concerned. They also (at least partly) reproduce the marked downslope decrease in velocities and kinetic energy (Sellmeier, 2015) that is induced by the (i) concave profile of the slope; (ii) energy absorption of rockfalls at each impact point, especially in the case of the first contacts (Bourrier and Hungr, 2013); and (iii)

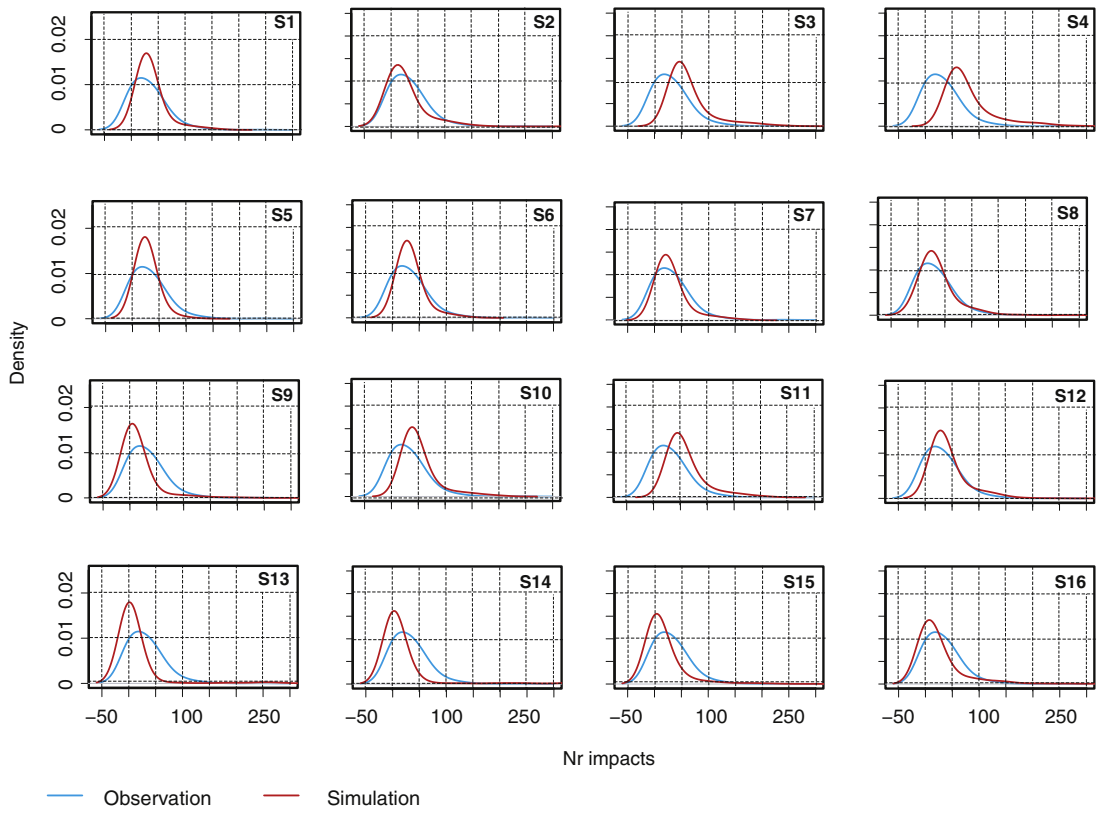

Fig. 8. Probability density functions of mean impact heights as observed at the study site (blue curve) and for simulations S1–S16 (red curves).

direct impact between a boulder and a trunk (Stokes, 2006; Dorren et al., 2007). Interestingly, despite different energy dissipation parameters, all convergent sets of simulations have low roughness values in common (Rg70 = 0, Rg20 < 0.05, and Rg10 < 0.10); whereas simulations S9–S16, characterized by higher *Rg* coefficients, generally fail to reproduce the distribution and the spatial patterns of observations. This lack of reproduction is mainly due to the underestimation of impact frequency in the lower half of the plot (cells F to L). In other words, in the latter simulations, obstacle height in the fall line prevents the falling blocks to travel far enough to result in recordable impacts in the lower part of the slope. In line with the study of Sellmeier (2015), who worked on limestone cliffs in the Bavarian Alps, this dichotomy demonstrates quite clearly that slight variations in roughness deeply affect the performance of rockfall runout modeling. It further confirms the sensitivity analysis of Dupire et al. (2016), realized on a virtual terrain, who demonstrated, for 0.5 m^3 blocks, a sharp decrease of runout distances in the range rg [0–15] cm. At our study site, a precise calibration of *Rg* values is even more crucial as (i) small block volumes ($0.4 \times 0.4 \times 0.4$ m^3) have been used for simulations and (ii) the impact of roughness changes on block propagation have been demonstrated to sharply increase with decreasing block diameter.

Yet, while the comparison of observed and modeled rockfall frequencies yielded very satisfactory results overall, the Kappa index (<0.22 also) revealed that the correspondence between predicted and observed numbers of tree hits remained quite poor at the cluster scale and in several sectors of the slope. First of all, stochastic elements - such as variations in the restitution coefficient (Bourrier et al., 2009; Gischig et al., 2015) - are involved in rockfall processes, such that a complete agreement of observed and simulated rockfalls is not unlikely to occur. In addition, the reasons for the discrepancies between model and observations also have to be accounted for different sources of errors.

Trappmann and Stoffel (2013) and Favillier et al. (2015) found differences in rockfall frequencies depending on the tree species investigated and the dating approach used. They noted that scar-count approaches might lead to an overestimation of past rockfall activity in trees with thin bark structures as these are likely to be more sensitive to damage. As a result, one rock may inflict multiple scars in one tree. At the same time, the very effective and rather rapid blurring of scars in certain other species with thick bark (Stoffel and Perret, 2006) may lead as well to an underestimation of rockfall activity at the same site.

A second source of discrepancies may from the method used to normalize the number of simulated impacts. Indeed, this normalization at the plot scale was used to render the number of impacts derived from the scar-counting and the modeling approaches comparable; but it can potentially lead to an overestimation of impacts, especially if scars are not scattered throughout the plot but clustered in its upper part (such as, e.g., in S9–S16).

A third factor includes the potential fragmentation of the released block during ground contacts (Giacomini et al., 2009; Wang and Tonon, 2011), a factor which is not currently incorporated in RockyFor3D but which could induce a dispersion of trajectories and subsequent impacts on trees along the falling path.

Finally, Corona et al. (2013) demonstrated that differences between simulated and observed numbers of tree impacts can be minimized through a careful definition of active source areas and a weighted distribution of block sizes as observed in the field. We thus believe that at our site spatial divergences between observations and simulations could result from (i) the automatic detection of source areas as well as from (ii) the use of a single block volume for all sets of simulations.

With regard to rockfall bounce heights, Stoffel et al. (2006) compared the results obtained with RockyFor3D with empirical data on tree impact heights in three mountain forests in Switzerland. In this pioneering study, the authors concluded that the model underestimated

mean impact heights observed on trees at the two sites where high-resolution input (DEM) and field data were available and overestimated them at the site where input and tree-ring data with the lowest resolution data were used. The authors concluded that the resolution of the DEMs, the delineation of rockfall source areas and initial fall heights, as well as the quality of the dendrogeomorphic data set would indeed explain the poor correspondence between the predicted and the observed mean impact heights. Similarly, in our analysis - based on a high-resolution DEM derived from airborne LiDAR data and an exhaustive analysis of 1495 impact height values observed on 1004 trees - the distribution of mean impact heights as derived with the scar-counting approach rarely converges with the distributions of bounce heights provided by the simulations (Table 2). These differences likely stem from the nature of the dendrogeomorphic data set. This data set, although unusually large for a rockfall slope, may not represent the full distribution of impact heights that is obtained from a very large number (e.g., release of 6,640,000 rocks causing between 28 and 567,523 tree impacts) of simulations (Bourrier et al., 2009). In addition, and as indicated by the generally low (<0.15) Cohen's K values, the poor agreement between observation simulation also points to the fact that rockfall models can only partly reproduce the patterns of observed impact heights. Yet, and provided a careful calibration of the energy dissipation and roughness parameters, significant improvement can be achieved between the distributions of mean impact heights obtained from field data and from the RockyFor3D simulations S2, S7, and S8. Finally, the best simulations, S1-S2, show a good convergence between observations and simulations with respect to the distribution and the pattern of impact frequencies and of impact height. They are based on (i) softer soil types that imply a loss of energy during each contact and hence a reduction in bounces and (ii) moderate roughness, which in turn enables the falling blocks to result in longer runout distances and hence recordable impacts in the lowermost parts of the slope.

6. Conclusions

In this study, an unusually dense and exhaustive dendrogeomorphic data set has been used to calibrate the 3D, physically based rockfall model RockyFor3D. Uncertainties related to energy dissipation and surface roughness have been investigated in detail as (i) both parameters are susceptible to affecting the energy loss of the falling block and their runout distance significantly. However, (ii) these parameters remain difficult to quantify and are usually estimated based on expert judgments. For this purpose, 16 scenarios that intersect four different soil types (corresponding to increasing values for the normal coefficient of restitution) have been used with four increasing roughness values. We were able to demonstrate that slight variations in roughness sharply affect the performance of runout modeling. In addition, we were also able to properly reproduce the decreasing downward propagation of rocks at our study site if obstacles of reduced size are used, thus enabling blocks to reach the lower parts of the plot. With respect to the height of impacts, differences between observed and simulated distributions can be minimized if moderate roughness values and softer soil types are applied as they limit bounces. Accounting for the sensitivity of rockfall modeling to input parameters, a combination of tree-ring analysis and modeling approaches should be used systematically wherever woody vegetation is available so as to reduce uncertainties and to increase the confidence and accuracy of modeling outputs.

Acknowledgements

This research has been supported by the National Research Project C2ROP (Chutes de blocs, Risques Rocheux, Ouvrages de Protection) supported by the MEDDE, French Ministry of Ecology, Sustainable Development and Energy (information available at http://www.c2rop.fr/). D.T and M.S. acknowledge financial support from the Swiss Federal Office for the Environment (FOEN, contract 15.0042.KP / O054-0339).

References

Agliardi, F., Crosta, G.B., Frattini, P., 2009. Integrating rockfall risk assessment and countermeasure design by 3D modelling techniques. Nat. Hazards Earth Syst. Sci. 9: 1059–1073. http://dx.doi.org/10.5194/nhess-9-1059-2009.

Astrade, L., Lutoff, C., Nedjaï, R., Philippe, C., Loison, C., Bottolier-Depois, S., 2007. Periurbanisation and natural hazards evolution of a mountainous area at an urban periphery and its inhabitants' awareness of natural hazards: The Lavanchon basin (Grenoble conurbation, France). J. Alp. Res. 95 (2), 19–28.

Bourrier, F., Hungr, O., 2013. Rockfall dynamics: a critical review of collision and rebound models. In: Lambert, S., Nicot, F. (Eds.), Rockfall Engineering. John Wiley & Sons, Inc., Hoboken, NJ, USA, pp. 175–209.

Bourrier, F., Dorren, L., Nicot, F., Berger, F., Darve, F., 2009. Toward objective rockfall trajectory simulation using a stochastic impact model. Geomorphology 110:68–79. http://dx.doi.org/10.1016/j.geomorph.2009.03.017.

Cardinali, M., Galli, M., Guzzetti, F., Ardizzone, F., Reichenbach, P., Bartoccini, P., 2006. Rainfall induced landslides in December 2004 in south-western Umbria, central Italy: types, extent, damage and risk assessment. Nat. Hazards Earth Syst. Sci. 6: 237–260. http://dx.doi.org/10.5194/nhess-6-237-2006.

Corominas, J., Moya, J., 2010. Contribution of dendrochronology to the determination of magnitude–frequency relationships for landslides. Geomorphology 124:137–149. http://dx.doi.org/10.1016/j.geomorph.2010.09.001.

Corona, C., Trappmann, D., Stoffel, M., 2013. Parameterization of rockfall source areas and magnitudes with ecological recorders: when disturbances in trees serve the calibration and validation of simulation runs. Geomorphology 202, 33–42.

Crosta, G.B., Agliardi, F., 2004. Parametric evaluation of 3D dispersion of rockfall trajectories. Nat. Hazards Earth Syst. Sci. 4:583–598. http://dx.doi.org/10.5194/nhess-4-583-2004.

Dorren, L.K.A., 2012. Rockyfor3D (v 5.0) revealed – transparent description of the complete 3D Rockfall Model. EcorisQ Pap. Assoc. EcorisQ St. Hilaire Touvet.

Dorren, L.K.A., Berger, F., le Hir, C., Mermin, E., Tardif, P., 2005. Mechanisms, effects and management implications of rockfall in forests. For. Ecol. Manag. 215:183–195. http://dx.doi.org/10.1016/j.foreco.2005.05.012.

Dorren, L.K.A., Berger, F., Putters, U.S., 2006. Real-size experiments and 3-D simulation of rockfall on forested and non-forested slopes. Nat. Hazards Earth Syst. Sci. 6:145–153. http://dx.doi.org/10.5194/nhess-6-145-2006.

Dorren, L., Berger, F., Jonsson, M., Krautblatter, M., Mölk, M., Stoffel, M., Wehrli, A., 2007. State of the art in rockfall – forest interactions. Schweiz. Z. Forstwes. 158:128–141. http://dx.doi.org/10.3188/szf.2007.0128.

Dupire, S., Bourrier, F., Berger, F., 2016. Predicting load path and tensile forces during cable yarding operations on steep terrain. J. For. Res. 21, 1–14.

Dussauge, C., 2003. Statistical analysis of rockfall volume distributions: implications for rockfall dynamics. J. Geophys. Res. 108. http://dx.doi.org/10.1029/2001JB000650.

Favillier, A., Lopez-Saez, J., Corona, C., Trappmann, D., Toe, D., Stoffel, M., Rovéra, G., Berger, F., 2015. Potential of two submontane broadleaved species (*Acer opalus*, *Quercus pubescens*) to reveal spatiotemporal patterns of rockfall activity. Geomorphology 246:35–47. http://dx.doi.org/10.1016/j.geomorph.2015.06.010.

Giacomini, A., Buzzi, O., Renard, B., Giani, G.P., 2009. Experimental studies on fragmentation of rock falls on impact with rock surfaces. Int. J. Rock Mech. Min. Sci. 46:708–715. http://dx.doi.org/10.1016/j.ijrmms.2008.09.007.

Gischig, V.S., Hungr, O., Mitchell, A., Bourrier, F., 2015. Pierre3D: a 3D stochastic rockfall simulator based on random ground roughness and hyperbolic restitution factors. Can. Geotech. J. 52:1360–1373. http://dx.doi.org/10.1139/cgj-2014-0312.

Hantz, D., Rossetti, J.P., Servant, F., 2014. Etude de la distribution des blocs dans un éboulement pour l'évaluation de l'aléa in Rock slope stability. 2-4 April 2014. Marrakech, p. 10.

Jaboyedoff, M., Labiouse, V., 2011. Technical note: preliminary estimation of rockfall runout zones. Nat. Hazards Earth Syst. Sci. 11:819–828. http://dx.doi.org/10.5194/nhess-11-819-2011.

Jaboyedoff, M., Dudt, J.P., Labiouse, V., 2005. An attempt to refine rockfall hazard zoning based on the kinetic energy, frequency and fragmentation degree. Nat. Hazards Earth Syst. Sci. 5:621–632. http://dx.doi.org/10.5194/nhess-5-621-2005.

Landis, J.R., Koch, G.G., 1977. The measurement of observer agreement for categorical data. Biometrics 33:159. http://dx.doi.org/10.2307/2529310.

Loye, A., Jaboyedoff, M., Pedrazzini, A., 2009. Identification of potential rockfall source areas at a regional scale using a DEM-based geomorphometric analysis. Nat. Hazards Earth Syst. Sci. 9:1643–1653. http://dx.doi.org/10.5194/nhess-9-1643-2009.

Matsuoka, N., Sakai, H., 1999. Rockfall activity from an alpine cliff during thawing periods. Geomorphology 28:309–328. http://dx.doi.org/10.1016/S0169-555X(98)00116-0.

Michoud, C., Derron, M.-H., Horton, P., Jaboyedoff, M., Baillifard, F.-J., Loye, A., Nicolet, P., Pedrazzini, A., Queyrel, A., 2012. Rockfall hazard and risk assessments along roads at a regional scale: example in Swiss Alps. Nat. Hazards Earth Syst. Sci. 12:615–629. http://dx.doi.org/10.5194/nhess-12-615-2012.

Perret, S., Stoffel, M., Kienholz, H., 2006. Spatial and temporal rockfall activity in a forest stand in the Swiss Prealps—a dendrogeomorphological case study. Geomorphology 74:219–231. http://dx.doi.org/10.1016/j.geomorph.2005.08.009.

Schneuwly, D.M., Stoffel, M., Dorren, L.K.A., Berger, F., 2009a. Three-dimensional analysis of the anatomical growth response of European conifers to mechanical disturbance. Tree Physiol. 29 (1247–125).

Schneuwly, D.M., Stoffel, M., Bollschweiler, M., 2009b. Formation and spread of callus tissue and tangential rows of resin ducts in Larix decidua and Picea abies following rockfall impacts. Tree Physiol. 29, 281–289.

Sellmeier, B., 2015. Quantitative Parameterization and 3D-run-out Modelling of Rockfalls at Steep Limestone Cliffs and the Bavarian Alps. Springer theses.

Smeeton, N.C., 1985. Early history of the kappa statistic. Biometrics 41, 795.

Stoffel, M., Corona, C., 2014. Dendroecological dating of geomorphic disturbance in trees. Tree-Ring Res. 70, 3–20.
Stoffel, M., Perret, S., 2006. Reconstructing past rockfall activity with tree rings: some methodological considerations. Dendrochronologia 24:1–15. http://dx.doi.org/10.1016/j.dendro.2006.04.001.
Stoffel, M., Wehrli, A., Kühne, R., Dorren, L.K.A., Perret, S., Kienholz, H., 2006. Assessing the protective effect of mountain forests against rockfall using a 3D simulation model. For. Ecol. Manag. 225:113–122. http://dx.doi.org/10.1016/j.foreco.2005.12.030.
Stoffel, M., Bollschweiler, M., Butler, D.R., Luckman, B.H., 2010. Tree Rings and Natural Hazards: A State-of-the-art. Springer, Heidelberg, Berlin, New York (505 pp.).
Stoffel, M., Butler, D.R., Corona, C., 2013. Mass movements and tree rings: a guide to dendrogeomorphic field sampling and dating. Geomorphology 200:106–120. http://dx.doi.org/10.1016/j.geomorph.2012.12.017.
Stokes, A., 2006. Selecting tree species for rockfall protection forests. For. Snow Landsc. Res. 80, 77–86.
Trappmann, D., Stoffel, M., 2013. Counting scars on tree stems to assess rockfall hazards: a low effort approach, but how reliable? Geomorphology 180-181:180–186. http://dx.doi.org/10.1016/j.geomorph.2012.10.009.
Trappmann, D., Stoffel, M., 2015. Visual dating of rockfall scars in *Larix decidua* trees. Geomorphology 245:62–72. http://dx.doi.org/10.1016/j.geomorph.2015.04.030.
Trappmann, D., Corona, C., Stoffel, M., 2013. Rolling stones and tree rings: a state of research on dendrogeomorphic reconstructions of rockfall. Prog. Phys. Geogr. 37: 701–716. http://dx.doi.org/10.1177/0309133313506451.
Trappmann, D., Stoffel, M., Corona, C., 2014. Achieving a more realistic assessment of rockfall hazards by coupling three-dimensional process models and field-based tree-ring data: assessment of rockfalls by coupling rockfall models and tree-ring data. Earth Surf. Process. Landf. 39:1866–1875. http://dx.doi.org/10.1002/esp.3580.
Volkwein, A., Schellenberg, K., Labiouse, V., Agliardi, F., Berger, F., Bourrier, F., Dorren, L.K.A., Gerber, W., Jaboyedoff, M., 2011. Rockfall characterisation and structural protection – a review. Nat. Hazards Earth Syst. Sci. 11:2617–2651. http://dx.doi.org/10.5194/nhess-11-2617-2011.
Wang, Y., Tonon, F., 2011. Discrete element modeling of rock fragmentation upon impact in rock fall analysis. Rock Mech. Rock. Eng. 44:23–35. http://dx.doi.org/10.1007/s00603-010-0110-9.